

Effect of Additives on Morphology Texture And Corrosion Resistance of Electrodeposited Zinc And Zinc-Cobalt Alloy

S.Selvakumari¹, M.Chandran¹, S.Premlatha², G.N.K.RameshBapu²,
P.Subramaniam³

¹Vivekananda college, Agasteeswaram, Kanyakumaridistrict, Tamilnadu - 62970, India

²CSIR-Central Electrochemical Research Institute, Karaikudi, Tamilnadu - 630006, India

³Aditanar college of arts and science, Tiruchendur, Tutucorin district, Tamilnadu - 628216, India

Corresponding Author:S.Selvakumari

Abstract: Zinc and Zinc –Cobalt alloy are widely used to protect iron and steel substrates against corrosion. In the present study, zinc and zinc – Cobalt alloys were electrodeposited from alkaline baths under incessant current and also in the presence of Vanillin (Vn), Saccharin (Sa), and Rochelle salt (Rs) as additives. AAS and EDAX show the coexistence of additives in the deposit. The deposit morphology has been analyzed using X-ray diffraction (XRD). Scanning Electron Microscopy (SEM) has been used to determine the favored crystallographic point of reference of the deposits. Studies have also been done on the CCE and Throwing power of zinc and zinc – cobalt alloy baths. The result shows that additives improve the nanostructure of the deposits hence, the corrosion resistance.

Keywords: Comparison of Zinc, Zinc – Cobalt alloys baths, CCE, Throwing power, AAS, EDAX. Morphology, XRD and Corrosion resistance

Date of Submission: 30-11-2017

Date of acceptance: 03-12-2017

I. INTRODUCTION

The sacrificial coating of zinc on to steel and other iron substrates is an effective and reliable standard of the industry for corrosion protection. The elements which are used successfully for alloying with zinc are iron, cobalt, nickel and tin. The important functions of alloying elements of iron, cobalt and nickel with zinc are usually used to modify the corrosion potential of the deposits. Zinc based material has very good corrosion resistance. Electrodeposited Zinc and Nickel alloys coatings are widely used in aerospace, electrical appliances, fasteners and as attractive coatings. The toxic nature of cadmium plating has been replaced by zinc-cobalt alloy plating [1-5]. Ramanauskas et al have reported that the morphology of Zn–Co alloy coatings plays a very important role in corrosion behavior of these coatings. Raeissi et al [6] have been investigated the texture and development of morphology during the electrodeposition of zinc and zinc–cobalt alloys. There are theories recommended by various researchers about anomalous co-deposition of zinc – cobalt alloy. The most accepted theory in this regard is hydroxide suppression mechanism. The acidic and alkaline plating baths are commonly used for the plating of zinc and zinc alloy deposits. The acidic baths revealed high current efficiency and high plating rate but have poor throwing power. The alkaline baths have shown uniform distribution of thickness but they have low current efficiencies. Zn–Co alloy has been electrodeposited from simple and complex baths. These electrodeposition methods produce anano sized grain structure with great advantages such as high invention rate, low cost and uniform deposition. Many researchers [7] have discussed that the zinc alloys provide good corrosion resistance than that of pure zinc. If zinc alloys have high amount of zinc, they can produce good protection than zinc alone, due to their sufficiently negative potential to steel. Bahrololoom et al. [8] have reported that more than 10 wt. % of cobalt content in bath of zinc–cobalt multilayer coatings have very good corrosion resistance than zinc–cobalt single layer coatings. In electrodeposition, the composition of bath, current density and temperature and pH obviously affect the microstructure and mechanical properties of the Zn–Co alloy. The commonly used additives in electroplating baths are classified as levelers and brighteners [9,10]. The presence of additives had great influence on zinc electrodeposition and they are morphological changes, refinement of grain size of deposit, formation of oriented grain structure [11] high throwing power, cathodic current efficiencies, and corrosion resistance. Synergistic interactions between additives have explained their important role of producing bright deposit [12,11,13]. The synergistic effect results have shown that the smoothening of zinc deposit produces at high current density could increases the current efficiency [14]. Tsuru et.al have been studied the nature of the solvent and its effect on Zn-Co co -deposition [15]. Glycines have been used to as a complexing agent in the electrodepositing of Zn-Co alloys [16]. The microstructure and morphology of the Co rich and Co–Zn alloys deposits were studied by Julyana et al. Bajat et al [17,18] have investigated the influence of various deposition current densities using Zn–Co alloys. H.Gharahcheshmehet al [19] have been studied the corrosion resistance of zinc and Zn–Co alloys from alkaline bath. The presence of additives has been

produced to an influence of the physical and mechanical properties from electrodeposits such as grain size, structure, brightness, internal stress, pitting and still the chemical composition and corrosion behavior. In this present study, electrodeposition of Zn–Co alloys has been carried out using alkaline bath. The bath composition, morphology and preferred crystallographic orientations of the deposits obtained in the absence and presence of Vanillin (Vn), Saccharin (Sa), and Rochelle salt (Rs) as additives have been analyzed and compared. The influences of additives are Vanillin (Vn), Saccharin (Sa), and Rochelle salt (Rs) on the plating process have also been discussed.

II. EXPERIMENTAL STUDIES

2.1. Electrolyte preparation

To optimize the bath composition, the Hull cell studies were made using 267 ml cell at current $I=1A/dm^2$ and duration $t = 5min$ [20]. The necessary pretreatments were given to the bath to remove metallic and organic impurities [21]. The solutions were freshly prepared from A.R grade reagents. Vanillin, Saccharin and Rochelle salt was used as additives for the present study. Pretreatment conditions were employed to mild steel prior to deposition. Mild steel of geometrical area $7.5 \times 2.5 \text{ cm}^2$ was polished successively with 1/0, 2/0, 3/0, 4/0, and 5/0 grade emery papers. Then it was degreased with trichloroethylene to remove the solid particles and washed with tap water followed by electrolytic cleaning. The electrolytic cleaning solutions were prepared by 35g/l of NaOH and 25g/l $NaHCO_3$ and the mild steel was immersed in solution for 2 minutes at $1 A/dm^2$. After electrolytic cleaning the plate was acid pickled in 10% H_2SO_4 and washed with distilled water.

2.2. Cathode Current Efficiency

The studies on current efficiency were carried out for different compositions of the electrolytes as decided in Hull cell experiments for different conditions of operation such as current density, temperature, pH and agitation. The electrodeposition assembly consists of two soluble zinc anodes and a steel cathode of equal size ($2.5 \times 7.5 \times 0.1 \text{ cm}$) dipped in one liter wide mouthed glass vessel. A regulated power supply was employed pH of the solution was measured by using digital pH meter. The specimens were weighed before and after deposition and the cathode current efficiency was calculated using the relation,

Cathode Current Efficiency (%) = $M \times 100 / M^1$

M - mass of the metal deposited
 M^1 - mass of metal deposited theoretically.

2.3. Throwing power

The Throwing power was measured employing a Haring – Blum cell [22]. The rectangular cell consists of two mild steel cathodes $3.0 \times 5.0 \times 0.1 \text{ cm}$ size filling the entire intersection at both ends and one perforated anode of the same size. If polarizable is negligible as compared with the potential drop in the electrolyte. The mass of the metal deposited on the nearer cathode (Cn) would be five times as much as that deposited on the farther cathode (Cf). Under such conditions, the electrolyte would behave in accordance with Ohm's law and the metal distribution would be proportional to the current distribution. The Haring – Blum formula for throwing power is given by

$$\text{Throwing power (\%)} = \frac{K - C}{K} \times 100$$

C = C_n/C_f is the metal distribution ratio between near and far cathode.

K- The ratio of the distance respectively of the farther and nearer cathodes from the anode. The modified Field's formula [23] is more realistic and range from +100% to -100% irrespective of the value of K.

$$\text{Throwing power (\%)} = \frac{K - C}{K + C - 2} \times 100$$

Throwing power was calculated for different solutions using Field's formula.

2.4. Atomic Absorption Spectroscopy

The elemental analysis of zinc and zinc cobalt alloy in the deposit with additives was carried out by Atomic Absorption Spectroscopic Technique based on Zeeman effect. The instrument is (Z-5000) polarized Zeeman atomic absorption spectrophotometer. Initially the alloy coated stainless steel samples were weighed (W1) accurately. Then the deposit were dissolved in a 5% Hydrochloric acid and made up to 100ml in a standard flask. After stripping of the deposit, the substrate was again weighed (W2) and the difference (W2-W1) gave the weight of deposit dissolved the concentration of zinc and zinc - cobalt alloy in the solution was analyzed by AAS. From the AAS results, the amount of Zinc and Cobalt was calculated as follows,

$$\% \text{ of Zinc in the deposit} = \frac{\text{weight of Zinc}}{\text{Total weight of the deposit}} \times 100$$

$$\% \text{ of Cobalt in the deposit} = \frac{\text{weight of cobalt}}{\text{Total weight of the deposit}} \times 100$$

2.5. Electro-deposits characterization

SEM photomicrographs of the deposits were obtained in absence and in presence of different addition agents used. The plated specimens were cut into (1cm²) size, mounted suitably and examined under the electron microscope SEM (JOEL-JEM-1200-EX I). X-ray diffraction patterns of the zinc and zinc –cobalt alloy with additives were recorded 15 Kv Hitachi, model S- 3000H (CECRI, Karaikudi) to determine the lattice parameter, crystallographic texture and approximate average grain size of the deposit. EDAX technique were carried out using 15 Kv Hitachi, model S- 3000H (CECRI, Karaikudi). It detects X –rays emitted from the sample during bombardment by an electron beam to characterize the elemental composition of the volume analysed.

2.6. Electrochemical corrosion measurement

The Linear polarization and Impedance studies were carried out in a conventional three-electrode cell. The working electrodes employed in voltammetric studies are mild steel disk of surface area 1 cm². The saturated calomel electrode (SCE) and a platinum wire were employed as reference and counter electrode respectively. Corrosion rate was measured using SP – 150 Bio Logic Science Instrument (CECRI , Karaikudi) the frequency range is 10mHZ to 100mHZ. For the optimized bath composition CCE, Throwing power, AAS has been studied at various current density from 0.5 to 3.0A/dm² for 15 minutes. The SEM, XRD, EDAX and Corrosion resistance have been carried with optimized bath composition. The pH of the bath solutions was maintained at pH 13.0.

III. Result And Discussion

3.1 Current Efficiency of zinc and zinc alloy deposit with additives

Fig: 1.1a shows the cathode current efficiency on zinc bath at various current densities (0.5 to 3 A/dm²). The CCE gradually increases with current density up to 2.0 A/dm² at 99.85% and decreases with further increasing current density. This is due to the hydrogen evolution occurring at the cathode along with zinc deposition at the high current densities. The zinc – cobalt alloy bath shows the effect of CCE in Fig: 1.1b. Fig: 1.1c shows the effect of current efficiency on zinc – cobalt alloy bath with additives. When Vanillin (1.0 g/l) is added at various current densities in alloy bath the CCE goes with 97.6% at 2.0 A/dm² and decreases with further increasing current density. This is also due the hydrogen evolution. In presence of combined additives of vanillin and saccharin at various current densities at (0.5 to 3 A/dm²), Fig. 1.1d the CCE values go on increasing at 2.0 A/dm² with 96.67% and decreasing with further increasing current density. The current efficiency of bath (v) solution was measured under plating conditions at various current densities in the fig: 1.1e. It was noticed that the CCE (0.5 to 3.0 A/dm²) increases up to 2.0 A/dm² at 97.87%. CCE values were gradually increasing with vanillin and rochelle salt compared to other additives. The synergistic effect of vanillin and rochelle salt is adsorption on the surface, but co-deposition in the case of zinc – cobalt alloy bath [24].

3.2. Variation of throwing power with current density

Values of throwing power of zinc and zinc-Cobalt alloy bath with additives. Fig. 2.2a shows throwing power of zinc bath (I) solution, at various current densities. Throwing power was found to be 56.5% to 86.3% for the current density variation from 0.5 to 3 A/dm². The zinc bath has throwing power of 29%. Results of the enhanced throwing power without additives on zinc – cobalt alloy bath when current density varied from 0.5 to 3 A/dm² are given in Fig. 2.2b. From the figure it can be noted that the throwing power varied from 63% to 83%. The enhanced the throwing power was by 20% in the case of zinc – cobalt alloy bath compared to zinc bath. Fig. 3.2 c shows the values of throwing power with additives on zinc- cobalt alloy bath at various current densities. The Throwing power obtained ranges from 71% to 95%. The enhanced throwing power using additives in the bath was by 24%. The variation of throwing power by use of combined additives on Zi – Co alloy bath was measured from 0.5 to 3 A/dm² and is shown the Fig. 2.2d. It can be noted that throwing power is from 45% to 80%. The combination of additives enhanced the throwing power by 33%. Fig 2.2e shows the change of throwing power on zinc- cobalt alloy bath with combined additives namely vanillin and rochelle salt. The throwing power was found to be 60% to 96% at various current densities from 0.5 to 3 A/dm². The combination of additives is found to have enhanced the throwing power of bath (V) by 36%, when compared to other additives.

3.3 Atomic Absorption Spectroscopic studies

From AAS study, the percentage values of zinc and zinc- cobalt alloy from combined additives during deposition on stainless steel cathode at various current densities with different temperatures are given in table 2. The stainless steel cathode deposit was stripped in 5% Hydrochloric acid solution. The zinc content in the stripped solution was analyzed using AAS. The percentage of zinc 99.83% up to 2.0 A/dm² and further

increasing current density, zinc percentage is decreased. The bath II solute on analysis gives the percentage of Zn (99.87%) & Co (0.115%) present in the alloy bath. The percentage of zinc increased in all baths, but cobalt showed very small increase percentage. Alloy bath (bath II) showed steep increase in the percentage of cobalt. Use of additives vanillin and rochelle salt (bath V) showed an increase in the percentage of zinc and cobalt compared to the bath of III and IV.

3.4. Morphological Studies

Figures 3.3a to 3.3e shows the Scanning Electron Microscopic studies of zinc and zinc-cobalt alloy deposits in presence of additives. The SEM images were recorded at 12 μ m (Fig: 3.3a). The surface morphology shows the random distribution of nano laminated plates. The SEM image of deposit obtained from zinc-cobalt alloy bath, appeared as tube like resemble structure (Fig 3.3b). Hexagonal rough surface has been observed for zinc-cobalt alloy with vanillin (Fig 3.3c). A hexagonal deposit has been observed for zinc-cobalt alloy with vanillin and saccharin (Fig: 3.3d). Fig 3.3e shows a fine grained size of deposit with uniform size for zinc-cobalt alloy deposit from bath with vanillin and rochellesalt.

3.5. EDAX Studies

The elemental composition of electrodeposited Zn-Co alloy with additives was determined with EDAX analysis and shown the Fig. 4.4a to 4.4e. The EDAX analysis of the deposits from bath I to bath V reveals that the deposits presence of zinc peaks have increased than the Co peaks as shown in table.3. The combined additives (bath V) have been increased percentage of zinc (103.28) and cobalt (2.09) than in the case of other deposit (bath I to bath IV) respectively.

3.6. XRD Analysis

The XRD patterns have been recorded to study the orientations of Zinc deposit obtained from zinc and zinc-cobalt alloy bath (Fig. 5 and Table 4 & 5). The average crystal size and the crystal orientation of the zinc and zinc-cobalt alloy with additives were analyzed using XRD as shown in fig 5. The XRD pattern for pure zinc deposit from bath I shows the average crystalline size 89nm and the characteristic diffracted peaks at $2\theta=44.03^\circ$ can be corroborated with the hexagonal platelets parallel to the electrode surface. Similar orientation were obtained for the deposit from bath II and the preferred crystal growth along (101) plane in zinc with the texture value of 100%. This shows the selective growth of grains with lowest surface free energy [25]. Hence (002) plane is generated in the absence of additives, assuming that the adsorbed hydrogen does not modify the metal surface energy. The Zn-Co alloy (bath II) deposit causes the growth of zinc and the texture coefficient is observed as 100% at peak $2\theta = 44.04^\circ$ and cobalt texture coefficient (63%) at peak $2\theta=44.04^\circ$ confirmed the formation of Zn-Co alloy on the (101) and (002) planes. Average crystal size obtained for Zn-Co alloy deposits are 59 nm and 89 nm respectively. As expected, characteristic peaks obtained for Zn-Co alloy deposits are broad showing smaller grain size of the coatings. The grain size of pure zinc is increased than that of Zn-Co alloy deposits suggested the importance of incorporated cobalt. The presence of vanillin (bath III) causes the preferred orientation of Zn-Co alloy (101) and (002) planes respectively. These observations are in good agreement with studied data ($2\theta = 43.03^\circ$) and average crystallite size is 59.6nm. In case of the deposit obtained from (bath IV) vanillin and saccharin the preferred orientation is same as in the case bath III and the hexagonal platelets are observed with average crystallite 59.5 nm. The combined additives vanillin and rochellesalt (bath V) generated less grain size and the preferred orientation is being along (101) and (002) planes respectively. The main peaks are at $2\theta = 43.63^\circ$ (Zn) and 43.21° (Co) confirms the presence of zinc and cobalt in the electrodeposits and the average crystallite size was calculated as 59 nm. The analysis using XRD technique shows the preferred orientation. It helps us to understand effect of additives on changes in microstructure of the deposit. The zinc deposit is formed by the electrochemical reduction of Zn^{2+} ions into Zn metal and consequent growth of Zn crystallites. The addition agent present in bath influences refinement in grain size surface roughness and preferred orientation of crystallites of the deposit.

3.7. Polarisation measurements

Fig 6 shows polarization curves during the deposition of the zinc and zinc-cobalt alloy with additives (bath I to V). The anodic and cathodic Tafel slopes during the polarization behavior of the deposited samples were found out. The exposed surface area was first scanned cathodically followed by anodic region, because in corrosion measurements only possible process in cathodic region is Hydrogen gas evolution. In zinc deposition (bath I), one can observe increment in I_{corr} and negative E_{corr} value. But current density is independent of potential [26,27]. In presence of cobalt on the zinc coating enhanced dissolution of zinc in 3.5% NaCl solution is the deposit from the zinc-cobalt alloy bath has higher protective ability compared that of zinc bath. In presence of additives (bath III to V), corrosion current density and corrosion potential are more negative E_{corr} and low current I_{corr} values determine the dissolution ability of materials. In the table.6 the chemical stability and corrosion resistance of metals are evaluated. The results show that when the corrosion potential decreases,

corrosion current also decreases. This trend is observed in case of all baths. The lowest value of I_{corr} is $8\mu\text{A}$ obtained for zinc – cobalt alloy deposited from the bath containing Rochelle salt and vanillin.

3.8. Impedance measurements

Fig 7. represents the Impedance analysis of zinc and zinc – cobalt alloy deposited from the bath with additives. The Nyquist Impedance curve was obtained for all baths (I to V) in 3.5% NaCl solution. These curves show a single semicircle at high frequencies. This can be attributed for the charge transfer controlled process. The diameter to the Nyquist diagram is correlated with higher charge transfer resistance (R_{ct}) and the equivalent circuit model consisting of double layer capacitance (C_{dl}). The results obtained are shown in Table. 7 and from the Impedance curves show significant difference in all coatings. The charge transfer resistance of zinc – cobalt alloy with Rochelle salt and vanillin show higher frequency than in the case of other coatings. It has significant corrosion resisting capability and compactness compared to other coatings. Thus, impedance results strongly support potentiodynamic polarization tests.

IV. CONCLUSIONS

1. The alkaline zinc and zinc – cobalt alloy bath exhibits better throwing power at current density studied will be useful for the new bath formulation in future.
2. The pH of the electrolyte does not have impact in alkaline solution.
3. The deposits from alkaline baths are fine grained with nano structure.
4. The higher over potential and smaller diffusion coefficient of zinc ions in presence of all additives indicate the combined interaction and adsorption of additives on electrode.
5. The higher over potential indicates the formation of more oriented (101) plane due to preferential adsorption of additives.
6. Deposits from the alloy bath with additives have higher corrosion resistance.
7. Zinc – Cobalt alloy deposit from the bath containing Rochellesalt and Vanillin has maximum corrosion resistance.

ACKNOWLEDGEMENT

The author (S. Selvakumari) expresses her sincere thanks to the Management, Vivekananda College, Agasteeswaram, Kanyakumari, for the encouragement given in her research pursuits.

REFERENCES

- [1]. Gabe DR, Green WA (1998) Surf Coat Technol 105:195
- [2]. Kalantary MR (1994) Plat Surf Finish 84:57
- [3]. Wilcox GD, Gabe DR (1994) Proceedings of Asian- Pacific Interfinish, Melbourne-2, Australian IMF, 50.1
- [4]. Crotty D, Griffin R (1997) Plat Surf Finish 84:57
- [5]. Short NR, Dennis JK (1997) Trans Inst Met Finish 75:47.
- [6]. K. Raeissi, A. Saatchi, M.A. Golozar, A. Tufani, J.A. Szpunar *Electrochimica Acta* 53 (2008) 4674-4678.
- [7]. R. Ramanauskas, L. Gudavicitute, R. Juskenas, *Chemija* 19 (1) (2008) 7-13.
- [8]. M.E. Bahrololoom, D. R. Gabe, and G. D. Wilcox, *Journal of Electroanalytical Chemistry* 421 (1997) 157-163.
- [9]. Shanmugasigamani, M. Pushpavanam, *J. Appl. Electrochem.* 36 (2006) 315-322.
- [10]. J.C. Hsieh, Chu-Chang, Tai-Chou Lee, *J. Electrochem. Soc.* 155 (2008) D675-D681.
- [11]. K.Boto, *Electrodeposition and Surface Treatment* 3 (1975) 77-95.
- [12]. N.D Nikolic, Z, Rakocevic, K.I. Popov, *J. Electroanal. Chem.* 514 (2001) 56-66.
- [13]. M. S Chandrasekar, Shanmugasigamani, M. Pushpavanam, *Mater. Chem. Phys.* 124(2010). 516-528.
- [14]. M.C. Li, Li Li Jiang, W.Q. Zhang, Y.H. Quian, Su Zhen Luo, JiaNianShen, *J. Solid State Electrochem.* 11 (2007) 549-553.
- [15]. 15. Arun Prasad, K. Giridhar.P, Ravindran.V, Muralidharan.V.S; *J. Solid State Electrochem.* 2001, 6, 63.
- [16]. Presuel – Moreno. F.J, Jakab. M.A., Scully. J.R., *J. Electrochem. Soc.* 2005, 152, B376.
- [17]. Julyana R. Garcia, Dalva C.B. do Lago, Deborah V. Cesar, Lilian F. Senna, *Surface & Coatings Technology* 20892 (2016) p.p.11.
- [18]. J.B. Bajat, S. Stankovic, B.M. Jokic , S.I. Stevanovic *Surface & Coatings Technology* 204 (2010) 2745-2753.
- [19]. M. HeydariGharahcheshmeh, M. HeydarzadehSohi, *Mater. Chem. Phys.* 117(2009) 414-421.
- [20]. L. Muresan, L. Oniciu, M. Froment, G. Maurin, *Electrochim. Acta* 37(1992)2249.
- [21]. A. Ramachandran and S.M. Mayanna. *Met. Finish.* 90 (1992) 61.

- [22]. H. Geduld. Zincate (or) Alkaline non – cyanide zinc plating in “zinc plating” (ASM International metals park, Ohio, (1988). PP.90 – 106.
- [23]. H. Silmen, G. Isserlis and A.F. Averill (Ed), ‘Preventive and decorative Coatings for Metals’, Finish in Publications Ltd., Teddington, England,(1978).
- [24]. M.S. Chandrasekar, Shanmugasigamani, M. Pushpavanam, Morphology and texture of pulse plated zinc-cobalt alloy, Mater. Chem. Phys. 115 (2009) 603-611.
- [25]. K. Saber, C.C. Koch, P.S. Fedkiw, Mater. Sci. Eng. A341 (2003) 174.
- [26]. P.D.L. Neto, A.N. Correia, R.P. Colares, W.S. Araujo, J. Braz. Chem. Soc. 18 (2007)1164–1175.
- [27]. K.M.S. Youssef, C.C. Koch, P.S. Fedkiw, Corros. Sci. 46 (2004) 51.

Table 1: Plating bath composition

Components	Bath I g/l	Bath II	Bath III g/l	Bath IV g/l	Bath V g/l
ZnO	10	10	10	10	10
NaOH	110	110	110	110	110
CoO	-	0.7	0.7	0.7	0.7
Vanillin	-	-	1.0	1.0	1.0
Saccharin	-	-	-	1.0	-
Rochellesalt	-	-	-	-	0.5

Table 2: Atomic Absorption Spectroscopic studies

Currentdensity (A/dm ²)	Bath I (%)	Bath II (%)		Bath III (%)		Bath IV (%)		Bath V (%)	
	Zn	Zn	Co	Zn	Co	Zn	Co	Zn	Co
0.5	99.89	99.93	0.097	99.97	0.028	99.95	0.056	99.97	0.026
1.0	99.88	99.91	0.107	99.95	0.040	99.95	0.069	99.96	0.050
1.5	99.85	99.89	0.108	99.94	0.068	99.94	0.058	99.96	0.035
2.0	99.83	99.87	0.115	99.93	0.085	99.94	0.067	99.95	0.048
2.5	99.82	99.84	0.112	99.92	0.072	99.93	0.059	99.94	0.050
3.0	99.81	99.82	0.111	99.91	0.089	99.92	0.072	99.93	0.067

Table 3: Elemental analysis

Sample	Quantitative analysis (%)				Total
	Zn	Co	C	O	
I	112.95	0	0	3.84	116.79
II	95.42	0.97	0	4.94	101.32
III	104.88	0	8.88	4.09	117.86
IV	93.22	0	0	7.99	101.21
V	103.28	2.09	0	5.26	110.62

Table 4: Texture coefficient (Tc) of zinc deposits

Plane (hkl)	Tc (Zn %) Standard	Tc (Zn %) Observed
(002)	37.1276	37.30
(100)	39.8159	19.59
(101)	44.0348	100
(110)	70.8279	17.32
(102)	55.1227	18.49
(103)	71.0335	9.51
(004)	77.8421	1.41

Table 5: Texture coefficient (Tc) of zinc and zinc-Cobalt alloy deposits

Plane (hkl)	Tc (Zn %) Standard	Tc (Zn %) Observed	Tc (Co %) Standard	Tc (Co %) Observed
(002)	37.1071	27.47	44.04	100
(100)	39.8266	21.11	-	-
(101)	44.0450	100	-	-
(110)	71.93	31	-	-
(102)	55.1227	18.49	55.2745	7.95
(103)	71.0335	9.51	-	-

Table 6: Polarisation data for bath I to V

Sample	Tafel slope (mv/ decade)		Ecorr (mv)	Icorr(µm)
	ba	bc		
I	71.8	71.6	-1149.46	30.449
II	92.9	48.4	-1211.659	25.013

III	83.5	50.8	-1189.865	16.989
IV	43.9	91.8	-1127.231	10.948
V	59.5	56.2	-1169.33	8.869

Table 7: Electrochemical Impedance data

Sample	Cdl	Rct
I	0.0543	292
II	0.811	404
III	0.54	607
IV	0.351	628
V	5.317	1364

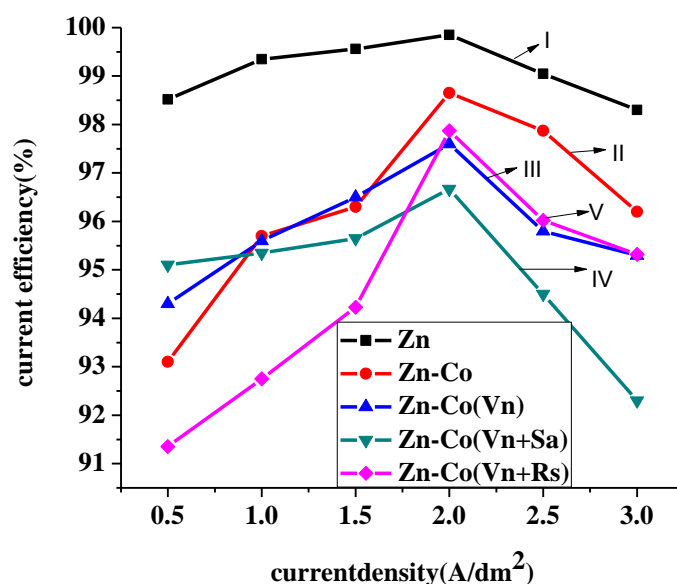


Fig. 1: Effect of current density on current efficiency of bath I to V at 30°C, pH – 13.

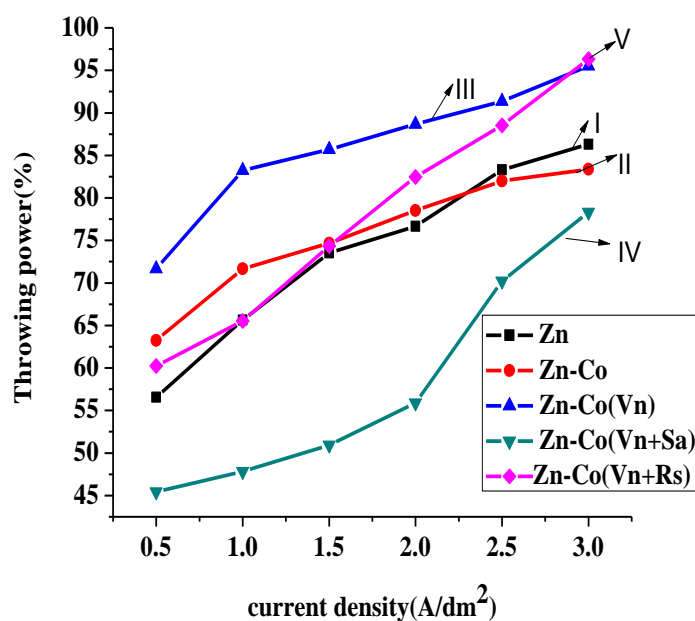


Fig. 2: Variation of throwing power on bath I to V, 30°C, pH – 13.

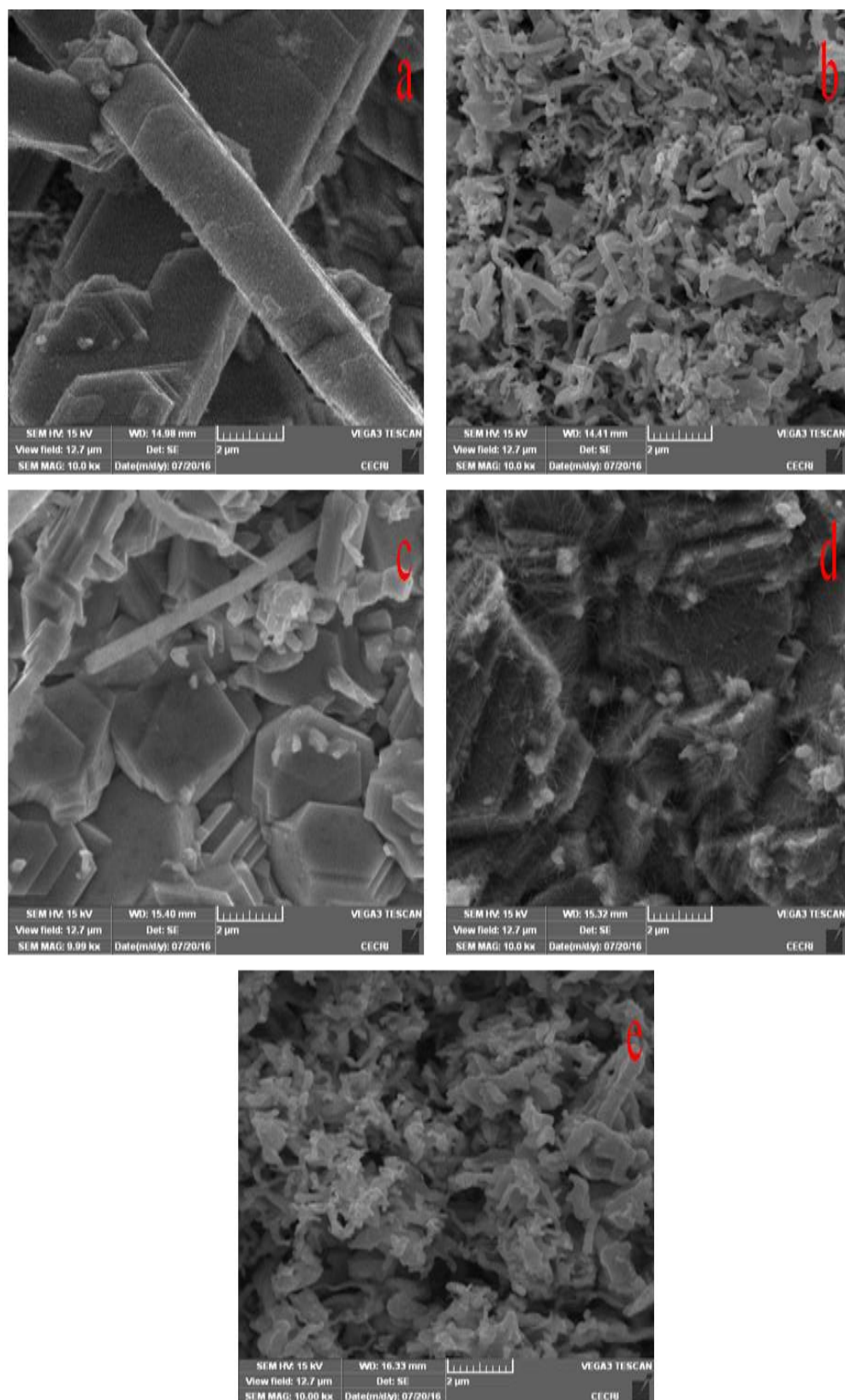
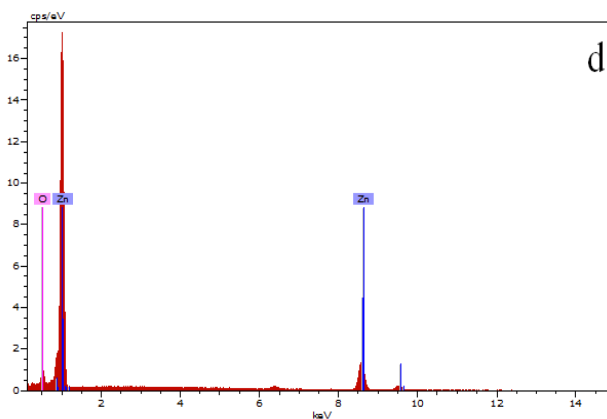
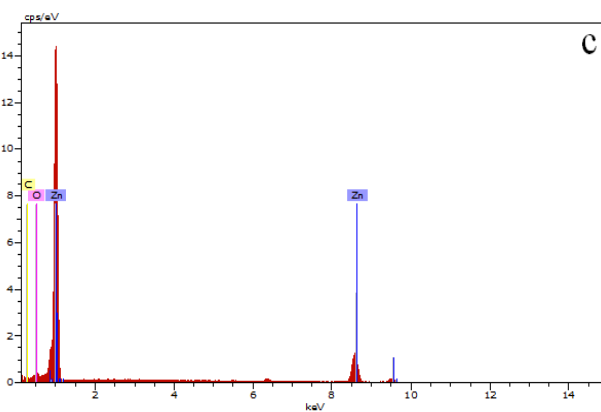
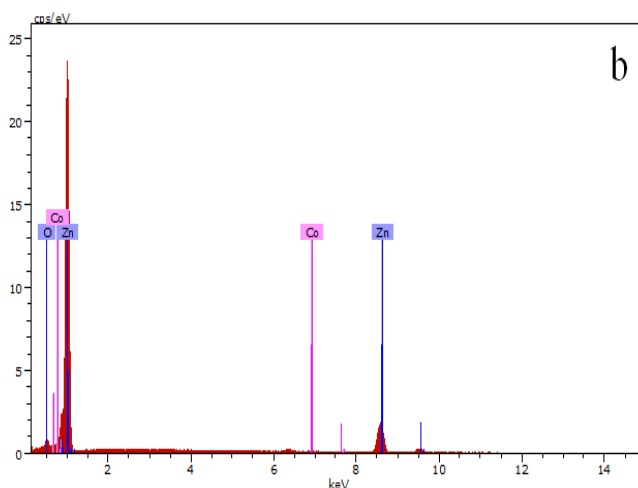
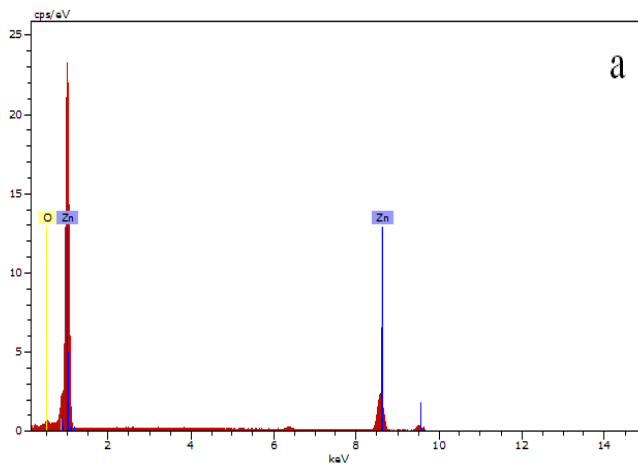


Fig. 3: SEM images of bath I (a), II (b), III (c), IV (d), and V (e) at 15 kx magnification



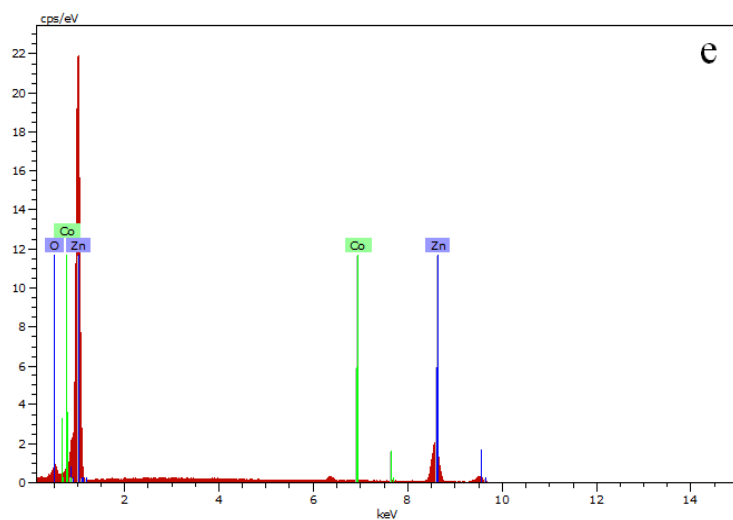


Fig. 4: EDAX patterns of bath I (a), II (b), III (c), IV (d), and V (e) at 12µm

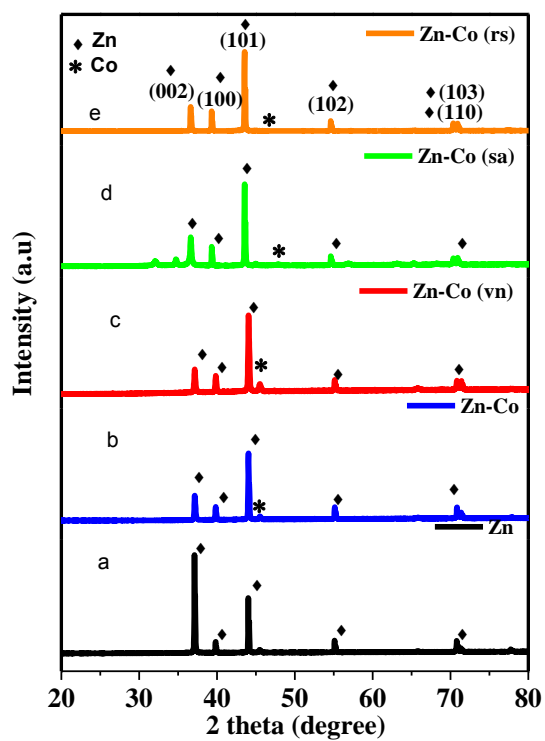


Fig. 5: XRD patterns of bath I (a), II (b), III (c), IV (d), and V (e) at 12 μ m

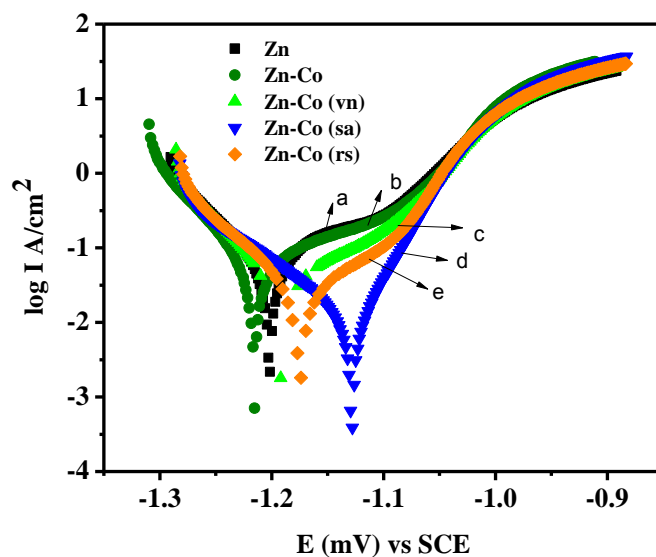


Fig. 6: Potentiodynamic Tafel plot of bath I (a), II (b), III (c), IV (d), and V (e) at 12 μ m

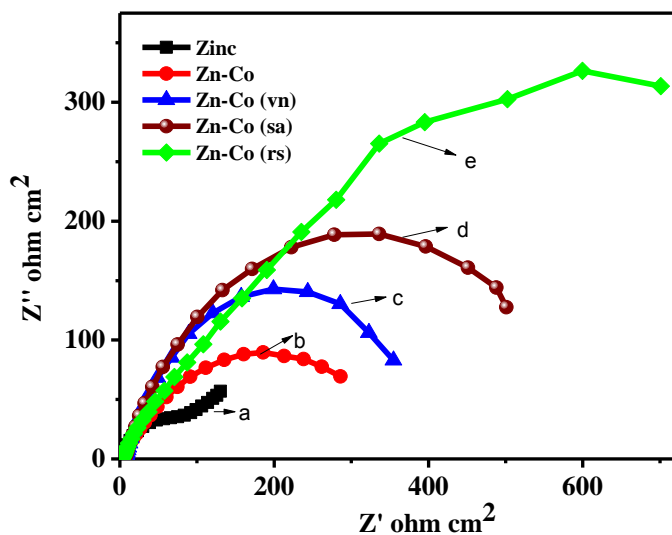


Fig. 7: Nyquist Impedance plot of bath I (a), II (b), III (c), IV (d), V (e) at 12 μ m

S.Selvakumari "Effect of Additives on Morphology Texture And Corrosion Resistance of Electrodeposited Zinc And Zinc-Cobalt Alloy." International Journal Of Engineering Research And Development , vol. 13, no. 12, 2017, pp. 21-31.